RESEARCH ARTICLE

Methane-cycling communities in a permafrost-affected soil on Herschel Island, Western Canadian Arctic: active layer profiling of *mcrA* and *pmoA* genes

Béatrice A. Barbier[1], Isabel Dziduch[1], Susanne Liebner[2], Lars Ganzert[2], Hugues Lantuit[1], Wayne Pollard[3] & Dirk Wagner[1]

[1]Alfred Wegener Institute for Polar and Marine Research, Research Unit Potsdam, Potsdam, Germany; [2]Department of Arctic and Marine Biology, University of Tromsø, Tromsø, Norway; and [3]Department of Geography, McGill University, Montréal, QC, Canada

Correspondence: Béatrice A. Barbier, Alfred Wegener Institute for Polar and Marine Research, Research Unit Potsdam, Telegrafenberg A43, 14473 Potsdam, Germany. Tel.: +49 331 288 2162; fax: +49 331 288 2188; e-mail: beatrice.barbier@awi.de

Received 27 October 2011; revised 8 February 2012; accepted 9 February 2012. Final version published online 8 March 2012.

DOI: 10.1111/j.1574-6941.2012.01332.x

Editor: Max Häggblom

Keywords
methanogens; methanotrophs; methane activity; T-RFLP; diversity.

Abstract

In Arctic wet tundra, microbial controls on organic matter decomposition are likely to be altered as a result of climatic disruption. Here, we present a study on the activity, diversity and vertical distribution of methane-cycling microbial communities in the active layer of wet polygonal tundra on Herschel Island. We recorded potential methane production rates from 5 to 40 nmol h^{-1} g^{-1} wet soil at 10 °C and significantly higher methane oxidation rates reaching values of 6–10 μmol h^{-1} g^{-1} wet soil. Terminal restriction fragment length polymorphism (T-RFLP) and cloning analyses of *mcrA* and *pmoA* genes demonstrated that both communities were stratified along the active layer vertical profile. Similar to other wet Arctic tundra, the methanogenic community hosted hydrogenotrophic (*Methanobacterium*) as well as acetoclastic (*Methanosarcina* and *Methanosaeta*) members. A pronounced shift toward a dominance of acetoclastic methanogens was observed in deeper soil layers. In contrast to related circum-Arctic studies, the methane-oxidizing (methanotrophic) community on Herschel Island was dominated by members of the type II group (*Methylocystis*, *Methylosinus*, and a cluster related to *Methylocapsa*). The present study represents the first on methane-cycling communities in the Canadian Western Arctic, thus advancing our understanding of these communities in a changing Arctic.

Introduction

Arctic permafrost environments play a crucial role in the global carbon cycle. Between 10 and 39 Tg a^{-1} of methane is released from permafrost environments, contributing up to 20% of global emissions (Cao *et al.*, 1998; McGuire *et al.*, 2009) and making them the largest single natural source of methane (Christensen *et al.*, 1996). Permafrost soils are also believed to contain 50% of the global belowground organic carbon pool (Tarnocai *et al.*, 2009), a considerable reservoir for potential future release of methane.

These environments are predicted to warm more rapidly than the rest of the globe (Anisimov *et al.*, 2007) and with them, the wet tundra ecosystems which host much of the methanogenic activity because of the water-logged, anoxic conditions that prevail in seasonally deepening thawed layers (Whalen & Reeburgh, 1992),

Methane release is in fact the net result between methanogenic and methanotrophic activity. Methane can be generated *in situ* by methanogenic archaea (a group belonging to the *Euryarchaeota*) under anaerobic conditions, but it can also be oxidized by methanotrophs such as methane-oxidizing bacteria (MOB), making tundra environments act as a methane sink (Whalen *et al.*, 1990; Callaghan *et al.*, 2005; Wagner & Liebner, 2009). MOB belong to the phylum Proteobacteria and can oxidize up to 90% of the methane emitted in the deeper layers before it reaches the atmosphere (Oremland & Culbertson, 1992; Le Mer & Roger, 2001; Wagner & Liebner, 2009). The balance between methane production and oxidation is thereby fragile and nonlinear as methanogens

and methanotrophs show a different response to temperature fluctuations (Ganzert *et al.*, 2007; Høj *et al.*, 2008; Knoblauch *et al.*, 2008; Liebner *et al.*, 2009).

Changing climate conditions could dramatically alter this balance and mobilize the large carbon pools found in permafrost, potentially creating a positive feedback loop with important global implications. Several studies have been conducted to explore this issue in Siberia (Kobabe *et al.*, 2004; Ganzert *et al.*, 2007; Wagner *et al.*, 2007; Liebner *et al.*, 2008; Dedysh, 2009), Svalbard (Wartiainen *et al.*, 2003; Høj *et al.*, 2008; Graef *et al.*, 2011) and the Canadian High Arctic (Pacheco-Oliver *et al.*, 2002; Martineau *et al.*, 2010; Yergeau *et al.*, 2010) to study the characteristics and dynamics of methane-cycling communities, but the communities of the Canadian Western Arctic remain unexplored to date.

In the following paper, the vertical distribution and diversity of two functional marker genes coding for enzymes involved in the methane cycle were investigated. To look at the diversity in the methanogenic population, we selected the gene coding for subunit A of the methyl coenzyme-M reductase enzyme (*mcrA*). Methyl coenzyme-M is the terminal enzyme complex in the methane generation pathway, methyl coenzyme-M reductase (MCR), which catalyzes the reduction of a methyl group bound to coenzyme-M, with the accompanying release of methane (Luton *et al.*, 2002). This enzyme complex is unique and ubiquitous in known methanogens (Thauer, 1998), and various studies have used it as a reliable tool for the specific detection of this group (Juottonen *et al.*, 2005; Steinberg & Regan, 2008; Biderre-Petit *et al.*, 2011).

To study the diversity of MOB, we selected the gene coding for subunit A of the particulate methane monooxygenase enzyme (*pmoA*). Methane monooxygenase (MMO) is found in either soluble or membrane-bound form, except in Methylocella species where only the membrane-bound form is present (Theisen & Murrell, 2005). MMO is responsible for the conversion of methane into methanol, which is either assimilated into biomass or oxidized to carbon dioxide (Semrau *et al.*, 1995).

Both functional genes are characterized by sufficient sequence divergence to serve as a reliable diagnostic gene for the study of the two populations of interest (McDonald & Murrell, 1997; Luton *et al.*, 2002).

In this study, we aimed to better understand the *in situ* dynamics between microbial-driven methanogenesis and methane oxidation in increasingly thawing permafrost. We calculated methane production and potential oxidation rates in an active layer soil profile from polygonal tundra on Herschel Island in the Canadian Western Arctic. To understand abiotic factors driving methane activity, we described the physico-chemical properties of the soil profile. We evaluated the assortment and distribution of *mcrA* and *pmoA* signatures throughout the soil profile using T-RFLP analysis. We complemented the fingerprinting results by constructing clone libraries of our two genes of interest. The results presented give new insights into the distribution and activity of methanogenic and methanotrophic microorganisms in the active layer of a rapidly degrading permafrost environment.

Materials and methods

Site description and sample collection

Active layer samples were collected from the 'Drained Lake' low-center polygon (N 69°34′43, W 138°57′25, elevation 30 m above sea level) on Herschel Island, Western Canadian Arctic (Fig. 1) during the expedition YUKON COAST in July–August 2010. A low-center polygon is an ice-wedge polygon in which thawing of ice-rich permafrost has left the central area in a relatively depressed position (van Everdingen, 2005). The soil at this site was characterized as a hemic glacistel classified according to the U.S. Soil Taxonomy (Soil Survey Staff, 1998) with poor drainage and a loamy soil texture. Vegetation cover included roughly 35% plant litter, 40% *Carex* sp. (sedges), 15% *Salix* sp. (dwarf willow), 10% mosses with traces of *Pedicularis* sp. (wooly lousewort), and *Ledum groenlandicum* (Labrador tea). The vegetation period spans yearly from mid-June to end of September. Average air temperatures vary annually between −26.3 °C in February to 8.7 °C in July (Burn & Zhang, 2009).

The sampling site was characterized by an active layer (the layer of ground that is subject to annual thawing and freezing) consisting of a large peat horizon, with a depth of 36 cm as measured using a permafrost probe. A hole was dug to the permafrost table, one side of the hole was cleaned, and blocks of soil were taken every 5 cm with a sharp sterile knife and placed into sterile 125 mL Nalgene® screw-cap containers (Thermo Fischer Scientific Inc., Waltham, MA). The knife was wiped down and sterilized with ethanol between different samples. Soil samples were frozen immediately after sampling and stored at −20 °C upon arrival in the laboratory. All subsequent subsampling was performed under sterile and anaerobic conditions in an atmosphere-controlled glove box.

Soil physico-chemical analyses

Gravimetric moisture content of soils was determined by weighing subsamples before and after freeze-drying for 72 h.

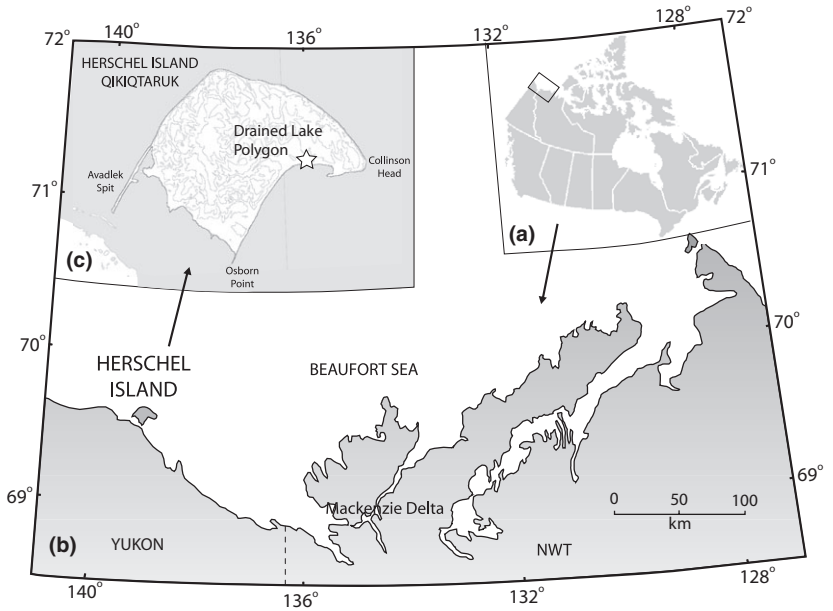

Fig. 1. Geographical location of study site (a) in Canada, (b) on the Yukon Coast and (c) Location of the Drained Lake Polygon on Herschel Island.

pH was measured using a CyberScan PC 510 Bench Meter (Eutech Instruments Pte Ltd, Singapore) following the slurry technique by mixing 1 : 2.5 mass ratio of samples and de-ionized water (Edmeades *et al.*, 1985).

Grain size was analyzed by first treating the samples with 30% H_2O_2 to digest all organic matter. After washing, the samples were freeze-dried and weighed. One per cent NH_3 solution was added to the samples and shaken for at least 24 h. Grain size was then measured at least twice for each sample with a Coulter LS 200 laser particle size analyser (Beckman Coulter, Brea, CA).

The percentage of total organic carbon (TOC) of the soils was measured in duplicate using a TOC analyzer (Elementar Vario max C, Germany). Samples prepared for analysis by freeze-drying and homogenized in an orbit mill ball-grinder (Pulverisette 5; Fritsch Ltd, Germany). The TOC content was calibrated using external standards of known elemental composition.

Water content, pH, and TOC could not be measured for the uppermost layer of the profile, as this mostly consisted of roots and plant material which were not sufficient to measure these parameters.

Methane measurements

Methanogenic activity of each soil layer was measured under simulated *in situ* conditions without substrate addition by placing 5 g of fresh soil material in 20 mL glass bottles and covered with 1 mL of sterile water under sterile, anaerobic conditions. The bottles were sealed with butyl rubber stoppers and flushed with N_2CO_2 (80 : 20% v/v). Triplicate samples were incubated in the dark at 10 °C. As a control, triplicate heat-sterilized samples were used. Samples were measured every 24 h for 1 week using an Agilent 6890 gas chromatograph (Agilent Technologies, Santa Clara, CA). Gases were separated on a Plot Q capillary column (0.53 mm diameter, 15 m length) using a gas flow of 30 mL min^{-1} with helium as carrier gas, and methane (CH_4) was measured through a flame-ionizing detector (FID). The oven and injector temperature were set at 80 °C and the detector temperature at 250 °C. All gas sample analyses were performed after calibration of the gas chromatograph with standard gases. CH_4 production rates were calculated from the linear increase in the CH_4 concentration in the headspace with time.

To study potential methane oxidation rates, fresh soil material (4 g) was placed in flat-walled culture bottles (50 mL) and distributed over the sidewall as a thin layer as described by Knoblauch *et al.* (2008). The bottles were sealed with butyl rubber stoppers and incubated horizontally. The headspace contained 2.5% v/v methane in synthetic air. Triplicate samples were incubated in the dark at 10 °C. Methane was measured repeatedly and the oxidation rates were calculated from the initial linear reduction in methane using multiple data points. Gas samples were measured in the same manner as described above. Heat-sterilized samples were used as the control.

Extraction of genomic DNA and PCR amplification

Total genomic DNA was extracted in duplicate from 0.6 g of soil using the PowerSoilTM DNA Isolation Kit (Mo Bio Laboratories, Carlsbad, CA) according to the manufacturer's protocol. Duplicates were then pooled for downstream analyses. Nucleic acids were eluted in 50 μL of elution buffer (MoBio). The concentration of the obtained genomic DNA was checked by spectrophotometry using a TrayCell (Hellma Analytics, Müllheim, Germany). DNA was then stored at −20 °C for further use in polymerase chain reaction (PCR) analyses.

PCR reactions were performed in triplicate 50 μL volumes containing between 10 and 50 ng of DNA, 0.5 μL of each 20 mM primer (forward primer labeled with the fluorescent dye carboxyfluorescein), 5 μL Q-Solution (Qiagen), 1.5 μL 10 mM dNTP mix, 5 μL 10× PCR buffer (Qiagen), 1 U of HotStar Taq DNA polymerase (Qiagen, Hilden, Germany), and PCR-grade water to 50 μL.

Primers used in the different PCR reactions are listed in Table 1. For the amplification of the archaeal *mcrA* gene, the primer pair MLf/MLr was used (Luton *et al.*, 2002). Reaction conditions were as follows: initial denaturation at 94 °C for 3 min, 35 cycles with denaturation at 94 °C for 25 s, annealing at 50 °C for 45 s, extension at 72 °C for 60 s, and a final extension at 72 °C for 5 min.

For the amplification of the methanotrophic *pmoA* gene, the primer pairs A189f/A682r and A189f/mb661r were used (Costello & Lidstrom, 1999; Holmes *et al.*, 1999) in a semi-nested PCR approach. The first PCR conditions were as follows: initial denaturation and polymerase activation at 95 °C for 5 min, 30 cycles with constant denaturation temperature at 94 °C for 45 s, decreasing annealing temperature from 62 to 52 °C for 60 s, elongation at 72 °C for 90 s, and final elongation at 72 °C for 90 s. The second PCR reaction conditions were initial denaturation and polymerase activation at 95 °C for 5 min, 22 cycles of denaturation at 94 °C for 45 s, annealing at 56 °C for 60 s, elongation at 72 °C for 90 s, and a final extension at 72 °C for 10 min.

Triplicate PCR reactions were visualized on a 1% agarose gel containing GelRed stain (Hayward, CA) and then purified using a QIAquick PCR Purification Kit (Qiagen). Purified PCR products were quantified by spectrophotometry using a TrayCell (Hellma Analytics).

Terminal restriction fragment length polymorphism (T-RFLP)

The digestion of fluorescently labeled PCR fragments using restriction enzymes was conducted in duplicate as follows. 10 U of enzyme MspI (Roche, Penzberg, Germany), 2 μL of 10× Buffer, and 500–600 ng of purified PCR product were mixed. PCR-grade water was added to 20 μL. The samples were then incubated for 3 h at 37 °C. The digestion was stopped by incubation at 80 °C for 20 min. Duplicate digests were pooled and purified using the QIAquick Purification Kit (Qiagen).

T-RFLP products (2 μL) were mixed with 0.25 μL of GeneScanTM 500 LIZ® internal size standard (Applied Biosystems, Darmstadt, Germany) and run on an ABI 3730xl DNA Analyzer (Applied Biosystems) at GATC Biotech (Konstanz, Germany). Afterward, the lengths of the fluorescently labeled terminal fragments (T-RFs) were visualized with Peak Scanner software (v1.0; Applied Biosystems).

T-RFLP results were analyzed statistically according to Dunbar *et al.* (2001) to yield relative abundance (%) of T-RFs. Briefly, T-RFs were aligned and clustered manually using Excel (Microsoft, Redmond, WA). DNA quantity between triplicate samples as well as between depth profiles was standardized in an iterative standardization procedure. For each sample, a derivative profile containing only the most conservative and reliable T-RF information was created by identifying the subset of T-RFs that appeared in all replicate profiles of a sample. Standardized, derivative profiles were then aligned. The average size of TRFs in each alignment cluster was calculated to produce a single, composite list of the T-RF sizes found among all samples. Relative signal intensity of each T-RF (%) was calculated based on the signal intensity of each individual T-RF with respect to the total signal intensity of all T-RFs in that sample. Peaks representing less that 1% of total fluorescence were eliminated from the profile to concentrate on the most representative microorganisms in each community. T-RFLP profiles were converted into

Table 1. Summary of properties of PCR primers used in this study

Primer	Target gene	Sequence (5′–3′)	Annealing T [°C]	References
A189f	*pmoA*	GGNGACTGGGACTTCTGG	52	Holmes *et al.* (1999)
A682r	*pmoA*	GAASGCNGAGAAGAASGC	52	Holmes *et al.* (1999)
mb661r	*pmoA*	CCGGMGCAACGTCYTTACC	56	Costello & Lidstrom (1999)
MLf	*mcrA*	GGTGGTGTMGGATTCACACARTAYGCWACAGC	50	Luton *et al.* (2002)
MLr	*mcrA*	TTCATTGCRTAGTTWGGRTAGTT	50	Luton *et al.* (2002)

presence–absence data and analyzed statistically by cluster analysis based on Bray–Curtis pairwise similarities using the software PRIMER 6 (Primer-E Ltd, Lutton, UK).

Cloning and sequence analyses

Based on the obtained T-RFLP results, various profile depths with the highest representative T-RF diversity (5–10 cm and 20–25 cm for *mcrA*; 0–5 cm and 15–20 cm for *pmoA*) were chosen to establish clone libraries. Libraries for the functional genes *mcrA* and *pmoA* were created by ligating PCR products into the pGEM-T Easy vector and transformed into competent cells *Escherichia coli* JM109 using the 'pGEM-T Easy Vector Systems II' Kit (Promega, Mannheim, Germany). White colonies containing inserts were picked, suspended in 1.2 mL of nutrient broth containing ampicillin (50 μg mL^{-1}), and grown overnight at 37 °C. Colonies were screened by PCR with vector primers M13 for correct size of the insert and the amplicons were directly sequenced by GATC Biotech AG. Ninety-six clones per gene were sequenced. The sequences were edited and contigs assembled using the SEQUENCHER software (v4.7; Gene Codes, Ann Arbor, MI). Nucleotide sequences were then screened and translated into correct amino acid sequences for further phylogenetic analyses using CLC sequence viewer software (version 6.5.1). Altogether, 81 McrA and 48 PmoA deduced amino acid (aa) sequences were used.

For McrA, sequences including nearest neighbors and cultured isolates were pre-aligned using the Muscle alignment tool integrated in MEGA 5 (Tamura *et al.*, 2011). The alignment was then imported in ARB (www.arb-home.de, Ludwig *et al.*, 2004) and manually checked. A neighbor-joining tree (Saitou & Nei, 1987) was constructed in ARB with a subset of 205 McrA amino acid sequences including nearest neighbors and representative isolate sequences (163 aa).

For PmoA, the deduced amino acid sequences were imported into an ARB database containing 3708 high quality PmoA sequences and were manually aligned. A neighbor-joining tree constructed in ARB with a subset of 127 PmoA sequences including nearest neighbors and representative isolate sequences (135 aa) using a 30% base frequency filter. The distance matrix was calculated using the neighbor-joining algorithm with a Kimura correction for McrA and a PAM correction for PmoA amino acid sequences. Rarefaction analysis was performed with DOTUR (Schloss & Handelsman, 2005) based on the furthest neighbor algorithm. Operational taxonomic units (OTUs) were defined using a 14.3% cutoff value for McrA according to Hunger *et al.* (2011) and a 7% cutoff for PmoA according to Degelmann *et al.* (2010).

Nucleotide sequence accession numbers

The environmental *mcrA* and *pmoA* clone sequences recovered in this study from the active layer of a polygon on Herschel Island were have been submitted to the GenBank nucleotide sequence databases and can be found under accession numbers JQ048956-JQ049081.

Results

Characteristics of the soil

The average *in situ* day temperature at the surface of the profile was 12 °C, decreasing gradually to −0.5 °C at the permafrost table (Fig. 2a). The pH of the entire profile was slightly acidic, ranging between 5.2 and 5.6 throughout (Fig. 2b). The mineral fraction of the soil represented only roughly 30%, as calculated after concentrated acid digestion of organic matter. The mineral fraction consisted on average of 27% sand, 20% silt, and 15% clay. The soil was visibly water saturated, with gravimetric moisture contents in the profile ranging from 77% near the surface and increasing to 83% close to the permafrost table (Fig. 2c). The organic carbon content was overall very high for all profile layers, ranging from 28% in the middle layers to 23% toward the permafrost table (Fig. 2d).

Methane production and oxidation

At an incubation temperature of 10 °C and with no added substrate, no significant methane production was found in the soil surface sample (0–5 cm depth) and only a low 1.4 nmol of CH_4 per hour and per gram of wet soil (nmol h^{-1} g^{-1}) was observed in the subsequent layer (Fig. 2e). The methanogenic activity in the deeper soil layers varied from 10.3 to 38.5 nmol h^{-1} g^{-1} with the exception of one sample (20–25 cm depth) where a lower value of 4.5 nmol h^{-1} g^{-1} was observed. The maximum potential methane production rates of 38.5 nmol h^{-1} g^{-1} occurred in the middle of the soil profile at 10–15 cm depth along with 35.8 nmol h^{-1} g^{-1} above the permafrost table at 30–35 cm depth.

The potential methane oxidation rate in the same profile varied between 43.5 and 9508.1 nmol h^{-1} g^{-1} (Fig. 2f). The maximum rate of 9.51×10^3 nmol h^{-1} g^{-1} was reached at 10–15 cm depth, at the same depth where the maximum methane production rate was also observed. High rates of 6.02×10^3, 6.66×10^3, and 3.368×10^3 nmol h^{-1} g^{-1} were observed in layers between 20 cm depth and the permafrost table.

Methane concentrations in the heat-sterilized controls did not increase during the incubation.

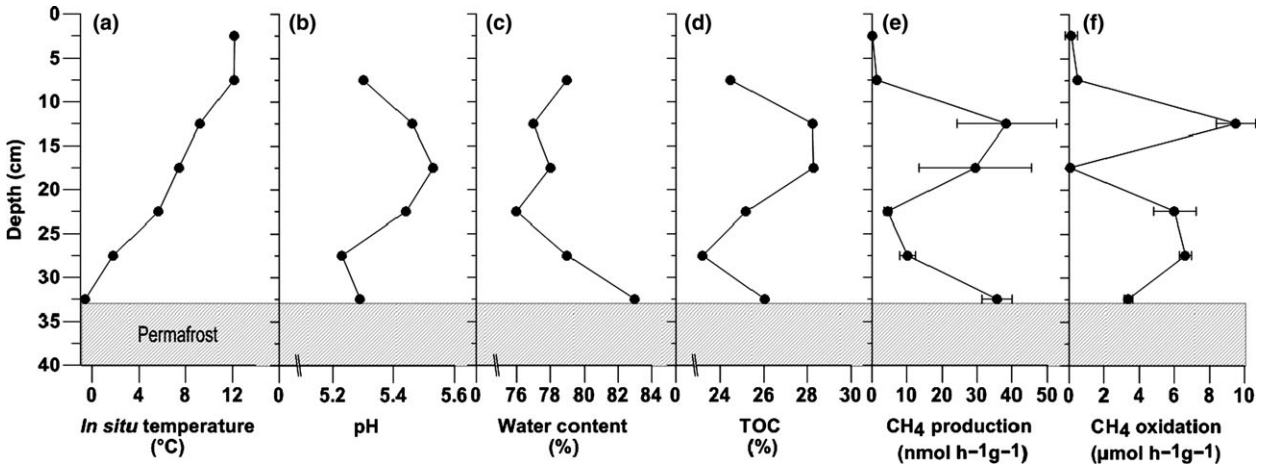

Fig. 2. Depth profile of abiotic and biotic parameters illustrating (a) active layer temperature as measured *in situ,* (b) soil pH, (c) percentage of water content, (d) percentage of total organic carbon in the soil (TOC), (e) potential methane production rate expressed in nanomol of methane per hour and gram of wet soil at 10 °C with no substrate addition, and (f) potential oxidation rate expressed in micromol of methane per hour and gram of wet soil at 10 °C in an atmosphere of 2.5% v/v methane in synthetic air. Error bars in (e) and (f) represent standard deviations.

Methanogenic and methanotrophic community structure

The community structure of methanogens and methanotrophs in the active layer profile was investigated through T-RFLP analysis of *mcrA* and *pmoA* functional genes (Fig. 3a,b). We obtained overall diverse communities, with a total of 17 T-RFs for the methanogenic archaea and 14 T-RFs for the methanotrophic bacteria.

Generally, we found that the methanogenic community became increasingly diverse with soil depth. No *mcrA* signal could be detected in the surface sample (Fig. 3a). Bray–Curtis similarity analysis of the *mcrA* T-RFLP data showed that community composition of methanogens was 80% similar between 15 and 36 cm depth. All samples taken together, excluding the surface layer, showed 60% similarity in community composition. The 5–10 cm depth sample displayed a different T-RF pattern compared with the subsequent depths, especially with respect to T-RF abundance. In this sample, the 463 bp T-RF represented 68% of total fluorescence, disappearing at the next sample depth and then reappearing in deeper layers, at a stable 10% of total T-RF abundance. A clear vertical shift in the community could be observed with predominating T-RFs in the surface layers (269, 272, 306 bp) decreasing in abundance in the deeper layers. The 269 bp T-RF could first be detected at 10–15 cm depth and represented between 35% and 55% of the community composition down to 35 cm depth. The 306 bp T-RF could first be detected at 5–10 cm depth and then gradually became more predominant in the community with increasing depth, making up 76% of the community close to the permafrost table.

The methanotrophic community based on *pmoA* showed the overall highest diversity in a depth between 10 and 30 cm of the active layer. Based on Bray–Curtis similarity analysis, the MOB community composition was heterogeneous throughout the different soil layers and samples clustered in a pairwise manner (Fig. 3b). Peaks of 245 and 246 bp clearly dominated the surface layers of the profile, representing 35% and 65%, respectively, of the total methanotrophic community between 0 and 10 cm depth. The T-RF of 117 bp first appeared at 10 cm depth and became progressively dominant in the profile with increasing depth. One T-RF of 100 bp was the only detectable peak close to the permafrost table. Overall, a shifting MOB community composition could be observed with increasing depth with T-RFs of 104, 117, 415, and 509 bp increasing in abundance while T-RFs of 245, 246 and 249 bp decreasing in abundance in the community profile.

Diversity and dominant species of *mcrA*

The clone library analysis of *mcrA* yielded a total of 85 cloned *mcrA* sequences. Four sequences resulting in < 100 amino acids were removed from further phylogenetic analyses. The diversity at the species level was low, resulting in six distinct OTU when using a cutoff value of 85.7% sequences similarity based on Hunger *et al.*, 2011 (Supporting Information, Fig. S1). Phylogenetic analyses of the clones indicated that the methanogenic community in the active layer profile was dominated by members of the genus *Methanobacterium* (1 OTU, 27 of 81 sequences), *Methanosarcina* (1 OTU, 19 sequences), *Methanosaeta* (1 OTU, 17 sequences), and *Methanocella*

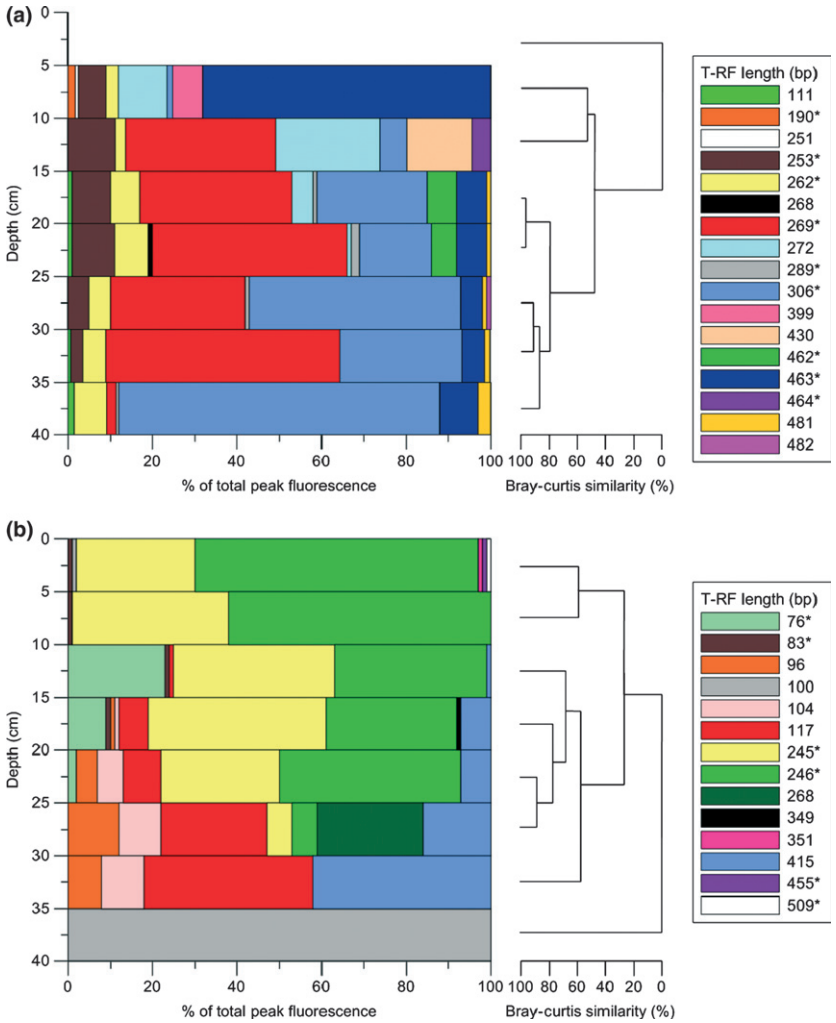

Fig. 3. Composition of methanogenic (a) and methantrophic (b) communities in an active layer profile on Herschel Island, Canada. Bars indicate the relative abundance of T-RFs of *mcrA* (a) and *pmoA* (b) functional gene amplicons. *mcrA*- and *pmoA*-based T-RFs obtained by enzymatic restriction using MspI. Numbers in the legend indicate the size of the T-RFs in base pairs (bp); an asterisk next to a T-RF size (e.g. 190*) indicates T-RFs for which a corresponding clone T-RF was found. Dendograms to the right of the histogram show similarity of T-RFLP profiles by Bray–Curtis hierarchical cluster analysis.

(1 OTU, 11 sequences). To a smaller extent, sequences related to the genus *Methanosphaerula* (1 OTU, six sequences) and only one sequence could be assigned to a novel, deep-branching group with relatives found in peat (Yrjälä *et al.*, 2011), a humic bog lake (Milferstedt *et al.*, 2010), Lake Pavin (Biderre-Petit *et al.*, 2011) and wetland soil (Narihiro *et al.*, 2011) (Fig. 4).

In an attempt to identify the most dominating methanogenic species in all depths of the active layer, T-RF sizes of 50 clones for *mcrA* were determined by digesting single clones with MspI, the same enzyme used for the whole-profile T-RFLP analysis. Clones from the sample library corresponded overall to nine T-RFs obtained in the whole community profile (Table 2, Fig 3a). Out of these eight T-RFs, two dominant fragments (269 and 306 bp) found in the overall profile corresponded to *Methanosarcina*. Two fragments (462, 463 bp) corresponded to *Methanobacterium*. The same fragment (463 bp) was also found to correspond to *Methanocella*. The remaining groups were represented by single T-RFs: *Methanosarcina*/*Methanosaeta* (253 bp), *Methanocella* (262 bp), and *Methanoregula* (289 and 464 bp). The numbers of clones found representing each T-RF along with their phylogenetic affiliation as obtained after comparison with the GenBank database using the BlastN algorithm are listed in Table 2.

Diversity and dominant species of *pmoA*

The clone library analysis of *pmoA* yielded a total of 65 cloned *pmoA* sequences. Based on a 7% cutoff for the

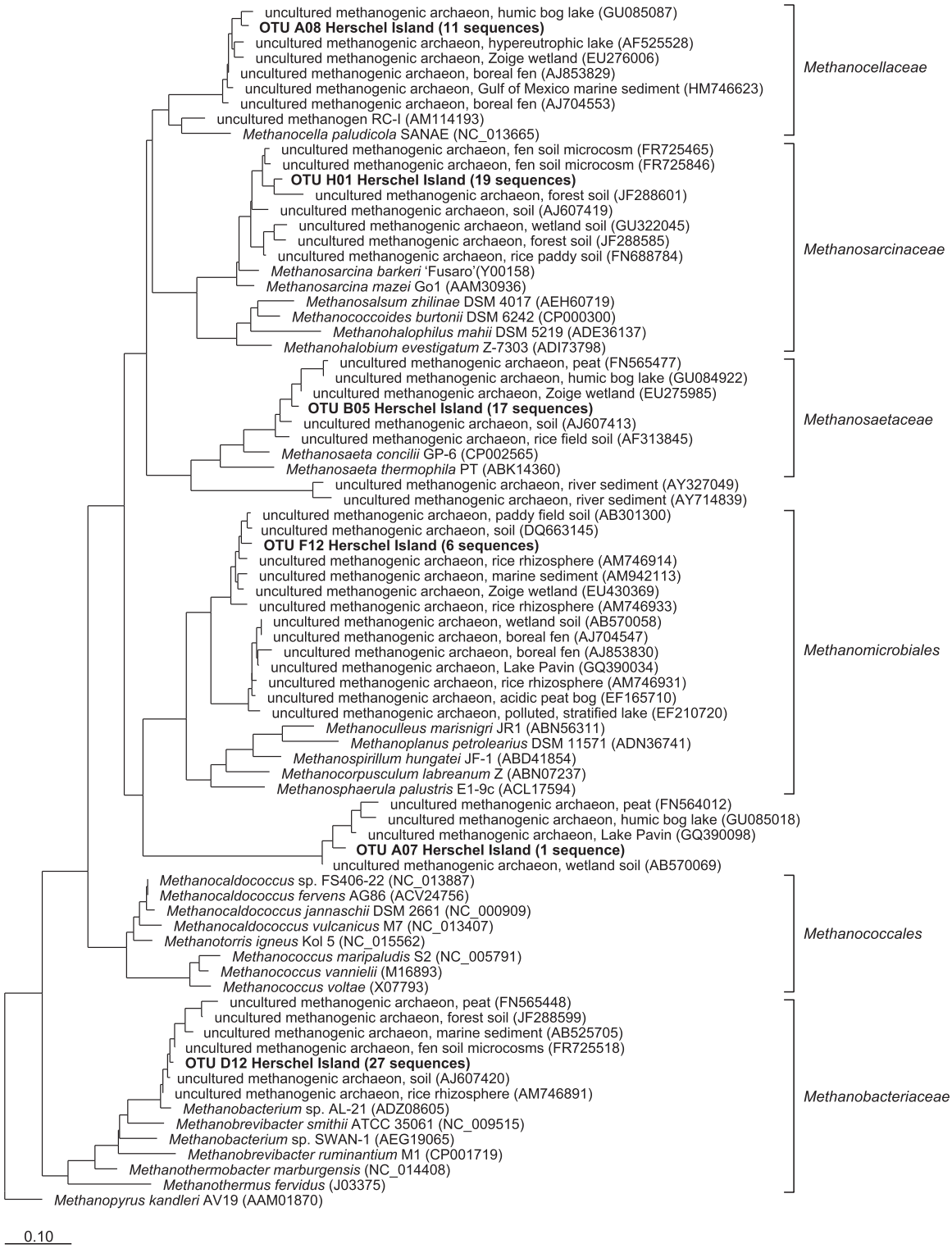

Fig. 4. Phylogenetic tree showing the relation of methanogen McrA amino acid sequences from active layer samples of Herschel Island, Canadian Western Arctic to known methanogen isolates and environmental sequences. The neighbor-joining tree was calculated from deduced amino acid sequences (159–163 aa) with *Methanopyrus kandleri* AV19 as outgroup. The 6 OTUs found in this study using a cutoff of 14.3% are in bold with the number of additional members that belong to the same OTU (in parentheses). The scale bar represents 0.10 changes per amino acid position.

Table 2. Phylogenetic assignment of active layer clones that matched the dominating soil T-RFLP peaks as obtained after comparison with the GenBank database using the BLASTN algorithm

T-RF size	Corresponding clone(s)	Accession number	Phylogenetic affiliation	Closest cultured relative	Accession number	Similarity (%)
mcrA						
190	mcrA-A07	JQ049004	*Methanomassiliicoccus*	*Methanomassiliicoccus luminyensis*	HQ896500.1	83
253	mcrA-D01	JQ049031	*Methanosarcina*	*Methanosarcina* sp. T36	AB288292.1	93
	mcrA-H03	JQ049073	*Methanosaeta*	*Methanosaeta concilii* GP-6	CP002565.1	85
262	mcrA-F10	JQ049058	*Methanocella*	*Methanocella paludicola* SANAE	AP011532.1	76
	mcrA-H04	JQ049074	*Methanocella*	*Methanocella paludicola*	AP011532.1	75
269	mcrA-E06	JQ582401	*Methanosarcina*	*Methanosarcina* sp. T36	AB288292.1	93
289	mcrA-C01	JQ049019	*Methanoregula*	Candidatus *Methanoregula boonei* 6A8	CP000780.1	83
306	mcrA-D06	JQ049035	*Methanosarcina*	*Methanosarcina* sp. T36	AB288292.1	92
	mcrA-E06	JQ582401	*Methanosarcina*	*Methanosarcina* sp. T36	AB288292.1	92
	mcrA-G01	JQ049061	*Methanosarcina*	*Methanosarcina* sp. T36	AB288292.1	92
462	mcrA-B12	JQ049018	*Methanobacterium*	*Methanobacterium* sp. AL-21	CP002551.1	90
	mcrA-C11	JQ049029	*Methanobacterium*	*Methanobacterium* sp. AL-21	CP002551.1	89
	mcrA-F09	JQ049057	*Methanobacterium*	*Methanobacterium* sp. AL-21	CP002551.1	89
	mcrA-E07	JQ049044	*Methanocella*	*Methanocella* sp. HZ254	JN081865.1	77
	mcrA-H06	JQ049076	*Methanocella*	*Methanocella* sp. HZ254	JN081865.1	76
463	mcrA-B12	JQ049018	*Methanobacterium*	*Methanobacterium* sp. AL-21	CP002551.1	90
	mcrA-C11	JQ049029	*Methanobacterium*	*Methanobacterium* sp. AL-21	CP002551.1	89
	mcrA-F09	JQ049057	*Methanobacterium*	*Methanobacterium* sp. AL-21	CP002551.1	89
	mcrA-E07	JQ049044	*Methanocella*	*Methanocella* sp. HZ254	JN081865.1	77
	mcrA-H06	JQ049076	*Methanocella*	*Methanocella* sp. HZ254	JN081865.1	76
464	mcrA-F12	JQ049060	*Methanoregula*	Candidatus *Methanoregula boonei* 6A8	CP000780.1	84
	mcrA-G12	JQ049070	*Methanoregula*	Candidatus *Methanoregula boonei* 6A8	CP000780.1	84
pmoA						
76	pmoA-C10	JQ048990	*Methylococcus*	*Methylococcus capsulatus*	AF533666.1	80
83	pmoA-E08	JQ048974	*Methylocystis*	*Methylocystis* sp. M212	JN036528.1	91
	pmoA-F04	JQ582402	*Methylocystis*	*Methylocystis* sp. M212	JN036528.1	91
245	pmoA-E08	JQ048974	*Methylocystis*	*Methylocystis* sp. M212	JN036528.1	91
	pmoA-F04	JQ582402	*Methylocystis*	*Methylocystis* sp. M212	JN036528.1	92
	pmoA-F05	JQ048976	*Methylosinus*	*Methylosinus* sp. LW2	AF150787.1	88
246	pmoA-A07	JQ582403	*Methylocystis*	*Methylocystis* sp. SS2C	AB636307.1	92
	pmoA-H01	JQ048981	*Methylocystis*	*Methylocystis* sp. M231	DQ852353.1	92
	pmoA-H04	JQ582404	*Methylocystis*	*Methylocystis parvus* strain OBBP	AF533665.1	92
	pmoA-C08	JQ582405	*Methylosinus*	*Methylosinus* sp. LW2	AF150787.1	93
455	pmoA-F02	JQ582406	*Methylocystis*	*Methylocystis* sp. SS2C	AB636307.1	92
509	pmoA-D03	JQ048967	*Methylosinus*	*Methylosinus* sp. LW2	AF150787.1	91
	pmoA-D02	JQ048966	*Methylocapsa*	*Methylocapsa acidiphila* B2	CT005238.2	79
	pmoA-A05	JQ048956	*Methylocapsa*	*Methylocapsa acidiphila* B2	CT005238.2	79

PmoA sequences (Fig. S1), 11 OTUs were defined with a clear dominance of type IIa methanotrophs (Fig. 5). A high proportion of sequences was affiliated to an uncultured *Methylocystis* cluster (3 OTUs, 17/48 sequences). Fifteen sequences (2 OTUs) clustered with uncultured *Methylosinus*/*Methylocystis*, eight sequences (3 OTUs) were affiliated with uncultured type Ia PmoA mainly from freshwater and mire habitats and which likely represents a new genus, seven sequences (2 OTUs) were affiliated to an uncultured cluster most closely related to *Methylocapsa* and a single sequence was most closely related to *Methylcystis* sp. 212 and related sequences from acidic and mire environments.

To identify the most dominating methanotrophic species in all depths of the active layer, T-RF sizes of 90 clones for *pmoA* were determined by digesting single clones with MspI. T-RFLP analysis of clones from the sample library corresponded to six T-RFs obtained in the whole community profile (Table 2, Fig. 3b). Out of these seven T-RFs, the two major fragments in the profile (245

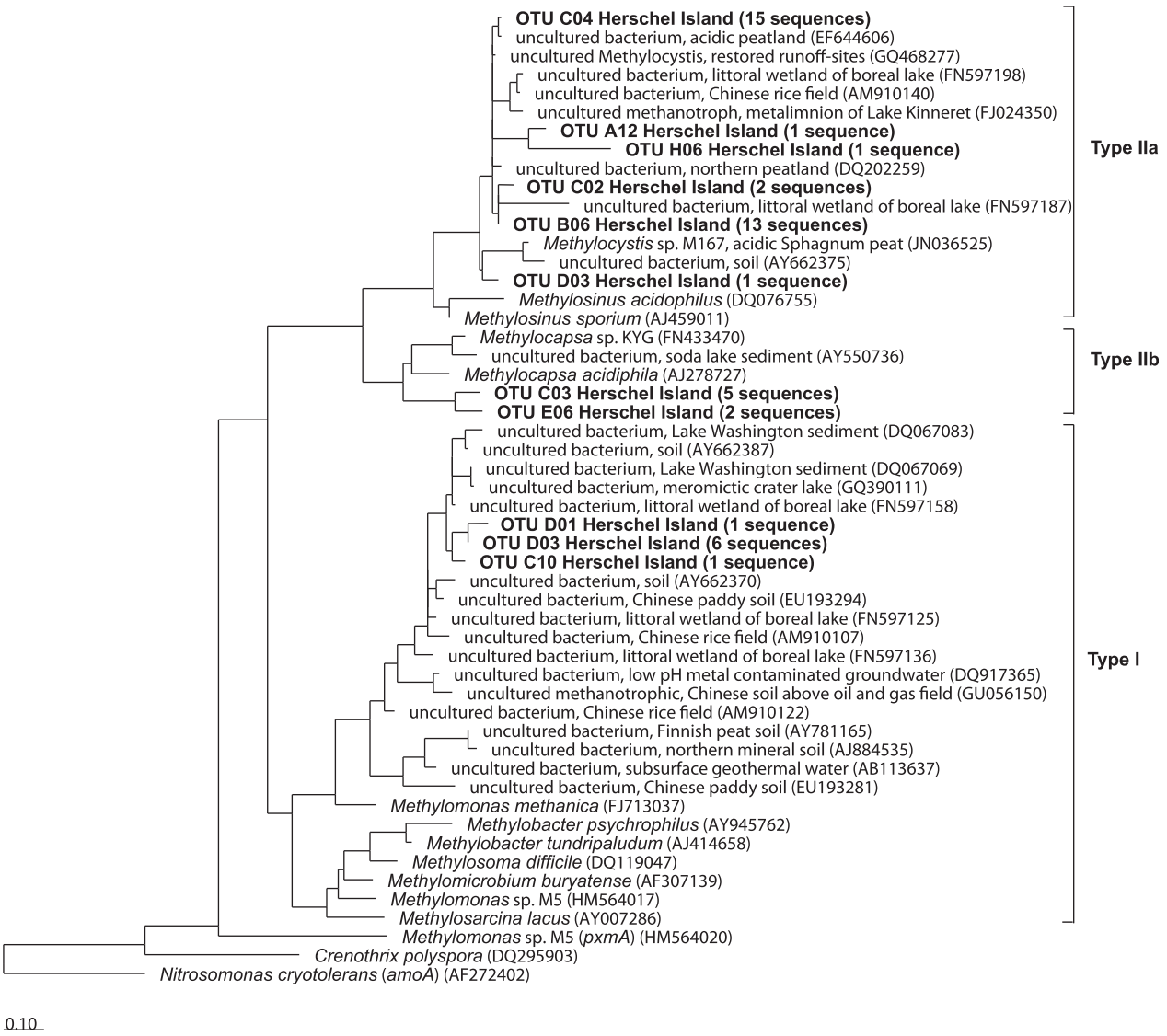

Fig. 5. Phylogenetic tree showing the relation of deduced MOB PmoA amino acid sequences from active layer samples of Herschel Island, Canadian Western Arctic to known MOB isolates and environmental sequences. The neighbor-joining tree was calculated from deduced amino acid sequences (135 aa) with *Nitrosomonas cryotolerans* as outgroup. The 11 OTUs found in this study using a cutoff of 7% are in bold with the number of additional members that belong to the same OTU (in parentheses). The scale bar represents 0.10 changes per amino acid position.

and 246 bp) corresponded to *Methylocystis* and *Methylosinus* and dominated the active layer profile between 0 and 25 cm depth. The 509 bp fragment found to correspond to *Methylocapsa* could only be detected to a small amount in the surface layer of the profile as well as between 15 and 20 cm depth. The 76 bp fragment with *Methylococcus* as the closest cultured relative was first detected in the middle of the active layer at 10 cm depth, decreasing in abundance down to 25 cm depth. The 83 bp fragment also corresponding to *Methylocystis* was detected at the same frequency in the upper half of the active layer.

The numbers of clones found representing each peak along with their phylogenetic affiliation as obtained after comparison with the GenBank database using the BlastN algorithm are listed in Table 2.

Discussion

Potential rates of methane production and methane oxidation

Although numerous studies have focused on surface methane fluxes in tundra environments in the circum-

Arctic region (e.g., Reeburgh *et al.*, 1998; Christensen *et al.*, 2003; Wille *et al.*, 2008), the microbiological communities behind these fluxes are still understudied. To understand the carbon fluxes from Arctic permafrost environments and the future development of these areas as a carbon source, it is essential to study the carbon dynamics and the microbial communities involved at different locations covering typical permafrost landscapes of the circum-Arctic. In this respect, the present study reported first results on the diversity of methane-cycling communities from a newly established environmental observatory in the Western Canadian Arctic.

It was shown that wet polygonal tundra environments on Herschel Island contained highly active methane-cycling communities. The highest potential methane production as well as oxidation rates at 10 °C in the vertical active layer profile was found in 10–20 cm soil depth, the second methane production optimum was found close to the permafrost table, while it appeared to be between 20 and 30 cm for methane oxidation. The observed potential methane production profile does not represent the typical activity pattern of methanogenesis in hydromorphic soils which would be no or little activity in the upper, oxic horizons and increasing rates in the anoxic bottom layers close to the permafrost table (Krumholz *et al.*, 1995). These methane production optima correlate with depths at which the organic carbon concentrations observed are at their highest throughout the profile, indicating a strong spatial correlation between the abundance of soil organic matter and methanogenesis as observed in previous studies in Siberia (Ganzert *et al.*, 2007). Methane oxidation rates correlated to or were just above depths at which the highest methanogenesis occurred, illustrating the close spatial location of methane production and oxidation in the studied active layer on Herschel Island. Methane production rates of 40 nmol CH_4 h^{-1} g^{-1} wet soil calculated in this study are comparable to those found *in situ* in other studies where rates of up to 39 nmol CH_4 h^{-1} g^{-1} wet soil were measured from the active layer of permafrost (Wagner *et al.*, 2003; Høj *et al.*, 2005; Metje & Frenzel, 2007). Potential methane oxidation rates in Siberian permafrost-affected soils were also calculated by Wagner *et al.* (2003) as well as in other studies (Liebner & Wagner, 2007; Knoblauch *et al.*, 2008), but the rates obtained in those studies (7–15 nmol CH_4 h^{-1} g^{-1} wet soil) were about three orders of magnitude smaller than the rate we calculated for active layer samples from Herschel Island. This could be due to differences in the activity and composition of the respective microbial communities. The activity of both processes is mainly affected by the water table position and the availability of substrates. It was shown for Siberian tundra that methane production activity decreased while oxidation rates increased concurrently with the progressing season (Wagner *et al.*, 2003). Although high methane oxidation rates can therefore be expected during the month of August, the potential methane oxidation rates calculated here are extremely high compared with what has been measured in similar arctic environments. They are rather similar to sub-Arctic rates as reported from a Finnish boreal mire (Jaatinen *et al.*, 2005) or a *Carex*-dominated fen in Alberta, Canada (Popp *et al.*, 2000). These high rates underline the importance of methanotrophic communities as the only terrestrial methane sink in Arctic wetlands (Trotsenko & Khmelenina, 2002), particularly with respect to permafrost degradation under future predicted global warming.

Structure of Herschel methane-cycling communities

Profiling *mcrA* and *pmoA* sequences along a permafrost-affected soil on Herschel Island, we extended the picture of methane-cycling communities in the Arctic and uncovered yet unseen microbial community composition in wet polygonal tundra. The MOB community found in the active layer of Herschel Island was more diverse than in other Arctic tundra environments and was dominated by type II organisms, primarily *Methylocystis*. Members of the *Methylocystis* genotype are known to thrive in methane-rich environments (Lüke *et al.*, 2010) but were not yet observed to dominate in Arctic tundra wetlands. Favorable conditions for type II methanotrophs in tundra soils were only reported for acidic *Sphagnum* peat where especially species of the genus *Methylocella* thrive (e.g., Dedysh *et al.*, 2004). However, *Methylocella* does not have a particulate methane monooxygenase and was not targeted in the present work. The MOB community on Herschel is thus unique for an Arctic tundra ecosystem and differs from what was reported until now in related studies on wet tundra of Siberia (Liebner *et al.*, 2008), Spitzbergen (Wartiainen *et al.*, 2003; Graef *et al.*, 2011) and the Canadian High Arctic (Martineau *et al.*, 2010). These studies consistently identified a dominance of type Ia methanotrophs and a generally very low diversity on the genus level (reviewed in Liebner & Wagner, 2010). In detail, we did not detect the presence of *Methylobacter tundripaludum* (Wartiainen *et al.*, 2006) or any other species of the *Methylobacter* genotype, although it was found to dominate in Arctic permafrost-affected soils of Svalbard where it was isolated (Wartiainen *et al.*, 2006; Graef *et al.*, 2011), Siberia (Liebner *et al.*, 2009) and the Canadian High Arctic (Martineau *et al.*, 2010) although a certain caution should be used when interpreting absences because of intrinsic uncertainties of the PCR reaction. Even so, these findings underline the uncommon composition of the MOB community in an Arctic environment.

In fact, the MOB community observed in this study is rather comparable to mire communities found in sub-arctic (Jaatinen *et al.*, 2005; Dedysh, 2009; Siljanen *et al.*, 2011) and temperate (Hoffmann *et al.*, 2002; Horz *et al.*, 2005; Chen *et al.*, 2008) ecosystems. Similarly, the extremely high potential methane oxidation rates observed here (discussed above) are comparable rather to what was reported in sub-arctic and temperate mires than in Arctic tundra soils (Jaatinen *et al.*, 2005; Liebner & Wagner, 2007). Given the slightly acidic pH and a mire-specific vegetation of our study site, the similarity to other mire MOB communities is not surprising. Soil temperature was also suggested to play a role in the establishment of either a type I or type II MOB community as described by Knoblauch *et al.* (2008) who observed a shift from a type I MOB community in Siberian permafrost-affected soils at low temperatures to an increase in type II MOB with increasing incubation temperature. The maritime climate and the higher annual average air temperature of −9.6 °C at our site on Herschel Island (Burn & Zhang, 2009) compared with −14.7 °C on Samoylov Island, Siberia (Wagner *et al.*, 2003), for example, could therefore have an influence in shaping the MOB toward a type II dominated community. These findings support the hypothesis that MOB communities are more sensitive to temperature variations (Liebner & Wagner, 2007), which could have implications in Arctic environments with respect to warming air temperatures and the weakening of MOB as a methane sink.

Methanogenic archaea are also known inhabitants of permafrost soils (reviewed in Wagner & Liebner, 2010). Our results indicate that hydrogenotrophic as well as acetoclastic methanogenesis occurs in active layer soils of the Western Canadian Arctic. Based on T-RFLP and sequence analyses, we found that the methanogenic archaea belonging to *Methanomicrobiales*, *Methanosarcina*, and *Methanosaeta* dominated in the active layer profile which has also been shown in other studies on archaeal diversity in Spitzbergen and Siberia (Høj *et al.*, 2005; Ganzert *et al.*, 2007). *Methanobacteria* that are hydrogenotrophic (Thauer, 1998) showed preferential colonization of the upper layer of the profile, its abundance quickly decreased with depth, while representatives of acetoclastic methanogens belonging to *Methanosarcina* and *Methanosaeta* (Thauer, 1998) were mainly found in the lower and colder soil layers. At low temperatures, there is a prevalence of the acetoclastic pathway of methanogenesis. Indeed, Conrad *et al.* (1987) showed that hydrogen-producing bacteria in paddy soils were inhibited at low temperatures, while homoacetogenesis is a dominant process in cold anoxic ecosystems (Nozhevnikova *et al.*, 1994). Hydrogenotrophic methanogenesis is hampered because of competition with acetogenic bacteria for hydrogen and carbon dioxide which produce acetate as a precursor for acetoclastic methanogens (Kotsyurbenko, 2005). Also, the availability of low molecular substances (e.g. acetate) provided by the root system of the vegetation (Chanton *et al.*, 1995; Ström *et al.*, 2003) could have an influence on the composition of the methanogenic community. Altogether, at the genus level, the community of methanogenic archaea observed here is representative of what has been found in other studies of permafrost soils (Høj *et al.*, 2005; Ganzert *et al.*, 2007; Metje & Frenzel, 2007). The low number of methanogenic OTUs in our study could be due to the low pH of the ecosystem. There are so far only a few cultured acidophilic methanogens known (Cadillo-Quiroz *et al.*, 2009; Bräuer *et al.*, 2011). This could also be due to substrate limitation even though the organic carbon concentration is high, as shown by Wagner *et al.* (2005). Indeed, methane emission rates and potential methane production in carbon-rich soils are dependent on substrate quality, which tends to decrease with the degree of decomposition (Ström *et al.*, 2003).

Based on T-RFLP fingerprints and Bray–Curtis analysis, we observed a vertical shift not only for methanogenic but also for methanotrophic communities. The surface layers clustered together and the respective community compositions of aerobic methane oxidizers were significantly different from those detected in layers closer to the permafrost table. In general, the active layer is a heterogeneous habitat in which biotic and abiotic factors, such as quantity and quality of soil organic matter, pH, soil temperature etc. vary along the soil profile (Fiedler *et al.*, 2004; Wagner *et al.*, 2005). Microbial communities close to the surface undergo large diurnal and seasonal temperature variations, influenced in the summer mainly by air temperature and solar radiation. The layers closer to the permafrost table, however, only vary by a few degrees and generally remain around 0 °C. Microorganisms close to the permafrost table are therefore more likely to be adapted to stable, cold *in situ* temperature as previously observed with methane-cycling communities in Sibera (Wagner *et al.*, 2003; Liebner *et al.*, 2009).

Conclusion

This study provides first insights into the methane-cycling microbial communities in a West Canadian permafrost soil on Herschel Island. We identified a methanotrophic community different from what was reported so far for Arctic tundra soils both in terms of community structure and potential activity. Comparative sequence analysis of uncultivated MOB revealed certain environmental distribution patterns and indicated an preference of specific genotypes to, for example, methane concentration or

salinity (Lüke *et al.*, 2010). Our results also illustrate that the composition of the MOB community in permafrost-affected soils is strongly influenced by environmental conditions such as low temperature and acidic pH. The community of methanogens was similar in composition to what we know from Arctic wet tundra and this community seems to be more stable in the circum-Arctic. We observed a clear shift from a hydrogenotrophic toward an acetoclastic community approaching the permafrost table. Such as shift, though, assumed to exist in tundra soils could never be shown so far.

Evaluating the results of this study in the scope of other studies from the Arctic, our present picture on circum-Arctic methane-cycling communities must still be considered as incomplete and biased toward the few studies conducted to date. It remains elusive whether methane-cycling communities which are specific to Arctic tundra environments truly exist.

Acknowledgements

The authors would like to thank three anonymous reviewers for their valuable comments and suggestions to improve the quality of this paper. We thank the German-Canadian field parties of the YUKON COAST 2010 expedition (Georg Schwamborn, Josefine Lenz, Michael Angelopoulos and David Fox) and the Herschel Island rangers for assistance with field measurements and sampling. Special thanks to Heather Cray (McGill University) for assistance with vegetation identification and to Richard Gordon (Parks Canada) for help with soil temperature measurements. We also thank Christiane Graef (University of Tromso) for valuable support for the phylogenetic analyses, Antje Eulenburg and Ute Bastian (Alfred Wegener Institute for Polar and Marine Research) for technical assistance and Juliane Bischoff (Alfred Wegener Institute for Polar and Marine Research) for critical reading of the manuscript. This study was funded by the 'International Cooperation in Education and Research' program of the International Bureau of the Germany Federal Ministry of Education and Research (BMBF) and through a doctoral scholarship to B.B. from the German Environmental Foundation (DBU). The authors declare no conflict of interest.

References

Anisimov OA, Vaughan DG, Callaghan TV, Furgal C, Marchant H, Prowse TD, Vilhjálmsson H & Walsh JE (2007b) Polar regions (Arctic and Antarctic). Climate change 2007: impacts, adaptation and vulnerability. *Contribution of Working Group II to the Fourth Assessment Report of the Intergovernmental Panel on Climate Change* (Parry ML, Canziani OF, Palutikof JP, van der Linden PJ & Hanson CE, eds), pp. 653–685. Cambridge University Press, Cambridge, UK.

Biderre-Petit C, Jézéquel D, Dugat-Bony E, Lopes F, Kuever J, Borrel G, Viollier E, Fonty G & Peyret P (2011) Identification of microbial communities involved in the methane cycle of a freshwater meromictic lake. *FEMS Microbiol Ecol* **77**: 533–545.

Bräuer SL, Cadillo-Quiroz H, Ward RJ, Yavitt JB & Zinder SH (2011) *Methanoregula boonei* gen. nov., sp. nov., an acidiphilic methanogen isolated from an acidic peat bog. *Int J Syst Evol Microbiol* **61**: 45–52.

Burn CR & Zhang Y (2009) Permafrost and climate change at Herschel Island (Qikiqtaruq), Yukon Territory, Canada. *J Geophys Res* **114**: F02001 16 pp. doi: 10.1029/2008JF001087.

Cadillo-Quiroz H, Yavitt JB & Zinder SH (2009) *Methanosphaerula palustris* gen. nov., sp. nov., a hydrogenotrophic methanogen isolated from a minerotrophic fen peatland. *Int J Syst Evol Microbiol* **59**: 928–935.

Callaghan TV, Björn LO, Chapin FS III *et al.* (2005) Arctic tundra and polar desert ecosystems. *Arctic Climate Impact Assessment* (Symon C, Arris L & Heal B, eds), pp. 243–352. Cambridge University Press, Cambridge.

Cao M, Gregson K & Marshall S (1998) Global methane emission from wetlands and its sensitivity to climate change. *Atmos Environ* **32**: 3293–3299.

Chanton JP, Bauer JE, Glaser PA, Siegel DI, Kelley CA, Tyler SC, Romanowicz EH & Lazrus A (1995) Radiocarbon evidence for the substrates supporting methane formation within northern Minnesota peatlands. *Geochim Cosmochim Acta* **59**: 3663–3668.

Chen Y, Dumont MG, McNamara NP, Chamberlain PM, Bodrossy L, Stralis-Pavese N & Murrell JC (2008) Diversity of the active methanotrophic community in acidic peatlands as assessed by mRNA and SIP-PLFA analyses. *Environ Microbiol* **10**: 446–459.

Christensen N, Bartuska A, Brown J *et al.* (1996) The report of the Ecological Society of America Committee on the scientific basis for ecosystem management. *Ecol Appl* **6**: 665–691.

Christensen TR, Ekberg A, Ström L *et al.* (2003) Factors controlling large scale variations in methane emissions from wetlands. *Geophys Res Lett* **30**: 1414.

Conrad R, Schütz H & Babbel M (1987) Temperature limitation of hydrogen turnover and methanogenesis in anoxic paddy soil. *FEMS Microbiol Ecol* **45**: 281–289.

Costello AM & Lidstrom ME (1999) Molecular characterization of functional and phylogenetic genes from natural populations of methanotrophs in lake sediments. *Appl Environ Microbiol* **65**: 5066–5074.

Dedysh S (2009) Exploring methanotroph diversity in acidic northern wetlands: molecular and cultivation-based studies. *Microbiology* **78**: 655–669.

Dedysh SN, Berestovskaya YY, Vasylieva LV, Belova SE, Khmelenina VN, Suzina NE, Trotsenko YA, Liesack W &

Zavarzin GA (2004) Methylocella tundrae sp. nov., a novel methanotrophic bacterium from acidic peatlands of tundra. *Int J Syst Evol Microbiol* **54**: 151–156.

Degelmann DM, Borken W, Drake HL & Kolb S (2010) Different atmospheric methane-oxidizing communities in European beech and Norway spruce soils. *Appl Environ Microbiol* **76**: 3228–3235.

Dunbar J, Ticknor LO & Kuske CR (2001) Phylogenetic Specificity and reproducibility and new method for analysis of terminal restriction fragment profiles of 16S rRNA genes from bacterial communities. *Appl Environ Microbiol* **67**: 190–197.

Edmeades D, Wheeler D & Clinton E (1985) The chemical composition and ionic strength of soil solutions from New Zealand topsoils. *Australian Journal of Soil Research* **23**: 151–165.

Fiedler S, Wagner D, Kutzbach L & Pfeiffer E-M (2004) Element redistribution along hydraulic and redox gradients of low-centered polygons, Lena Delta, Northern Siberia. *Soil Sci Soc Am J* **68**: 1002–1011.

Ganzert L, Jurgens G, Münster U & Wagner D (2007) Methanogenic communities in permafrost-affected soils of the Laptev Sea Coast, Siberian Arctic, characterized by 16S rRNA gene fingerprints. *FEMS Microbiol Ecol* **59**: 476–488.

Graef C, Hestnes AG, Svenning MM & Frenzel P (2011) The active methanotrophic community in a wetland from the High Arctic. *Environ Microbiol Rep* **3**: 466–472.

Hoffmann T, Horz H-P, Kemnitz D & Conrad R (2002) Diversity of the particulate methane monooxygenase gene in methanotrophic samples from different rice field soils in china and the philippines. *Syst Appl Microbiol* **25**: 267–274.

Høj L, Olsen RA & Torsvik VL (2005) Archaeal communities in High Arctic wetlands at Spitsbergen, Norway (78°N) as characterized by 16S rRNA gene fingerprinting. *FEMS Microbiol Ecol* **53**: 89–101.

Høj L, Olsen RA & Torsvik VL (2008) Effects of temperature on the diversity and community structure of known methanogenic groups and other archaea in high Arctic peat. *ISME J* **2**: 37–48.

Holmes AJ, Roslev P, McDonald IR, Iversen N, Henriksen K & Murrell JC (1999) Characterization of methanotrophic bacterial populations in soils showing atmospheric methane uptake. *Appl Environ Microbiol* **65**: 3312–3318.

Horz H-P, Rich V, Avrahami S & Bohannan BJM (2005) Methane-oxidizing bacteria in a california upland grassland soil: diversity and response to simulated global change. *Appl Environ Microbiol* **71**: 2642–2652.

Hunger S, Schmidt O, Hilgarth M, Horn MA, Kolb S, Conrad R & Drake HL (2011) Competing formate- and carbon dioxideutilizing prokaryotes in an anoxic methane-emitting fen soil. *Appl Environ Microbiol* **77**: 3773–3785.

Jaatinen K, Tuittila ES, Laine J, Yrjälä K & Fritze H (2005) Methane-oxidizing bacteria in a finnish raised mire complex: effects of site fertility and drainage. *Microb Ecol* **50**: 429–439.

Juottonen H, Galand PE, Tuittila ES, Laine J, Fritze H & Yrjälä K (2005) Methanogen communities and *Bacteria* along an ecohydrological gradient in a northern raised bog complex. *Environ Microbiol* **7**: 1547–1557.

Knoblauch C, Zimmermann U, Blumenberg M, Michaelis W & Pfeiffer EM (2008) Methane turnover and temperature response of methane-oxidizing bacteria in permafrost-affected soils of northeast Siberia. *Soil Biol Biochem* **40**: 3004–3013.

Kobabe S, Wagner D & Pfeiffer E-M (2004) Characterisation of microbial community composition of a Siberian tundra soil by fluorescence *in situ* hybridisation. *FEMS Microbiol Ecol* **50**: 13–23.

Kotsyurbenko OR (2005) Trophic interactions in the methanogenic microbial community of lowtemperature terrestrial ecosystems. *FEMS Microbiol Ecol* **53**: 3–13.

Krumholz LR, Hollenback JL, Roskes SJ & Ringelberg DB (1995) Methanogenesis and methanotrohpy within a Sphagnum peatland. *FEMS Microbiol Ecol* **18**: 215–224.

Le Mer J & Roger P (2001) Production, oxidation, emission and consumption of methane by soils: a review. *Eur J Soil Biol* **37**: 25–50.

Liebner S & Wagner D (2007) Abundance, distribution and potential activity of methane oxidising bacteria in permafrost soils from the Lena Delta, Siberia. *Environ Microbiol* **9**: 107–117.

Liebner S & Wagner D (2010) Permafrost – Current and future challenges to study methanotrophy in permafrost affected tundra and wetlands. *Handbook of Hydrocarbon and Lipid Microbiology* (Timmis KN, ed), pp. 2173–2179. Springer-Verlag, Berlin, Heidelberg, Germany.

Liebner S, Harder J & Wagner D (2008) Bacterial diversity and community structure in polygonal tundra soils from Samoylov Island, Lena Delta, Siberia. *Int Microbiol* **11**: 195–202.

Liebner S, Rublack K, Stuehrmann T & Wagner D (2009) Diversity of aerobic methanotrophic bacteria in a permafrost active layer soil of the Lena Delta, Siberia. *Microb Ecol* **57**: 25–35.

Ludwig W, Strunk O, Westram R *et al.* (2004) ARB: a software environment for sequence data. *Nucleic Acids Res* **32**: 1363–1371.

Lüke C, Krause S, Cavigiolo S, Greppi D, Lupotto E & Frenzel P (2010) The biogeography of wetland rice methanotrophs. *Environ Microbiol* **12**: 862–872.

Luton PE, Wayne JM, Sharp RJ & Riley PW (2002) The *mcrA* gene as an alternative to 16S rRNA in the phylogenetic analysis of methanogen populations in landfill. *Microbiology* **148**: 3521–3530.

Martineau C, Whyte LG & Greer CW (2010) Stable isotope probing analysis of the diversity and activity of methanotrophic bacteria in soils from the Canadian High Arctic. *Appl Environ Microbiol* **76**: 5773–5784.

McDonald IR & Murrell JC (1997) The particulate methane monooxygenase gene *pmoA* and its use as a functional gene probe for methanotrophs. *FEMS Microbiol Lett* **156**: 205–210.

McGuire AD, Anderson LG, Christensen TR, Dallimore S, Guo L, Hayes DJ, Heimann M, Lorenson TD, Macdonald RW & Roulet N (2009) Sensitivity of the carbon cycle in the Arctic to climate change. *Ecol Monogr* **79**: 523–555.

Metje M & Frenzel P (2007) Methanogenesis and methanogenic pathways in a peat from subarctic permafrost. *Environ Microbiol* **9**: 954–964.

Milferstedt K, Youngblut ND & Whitaker RJ (2010) Spatial structure and persistence of methanogen populations in humic bog lakes. *ISME J* **4**: 764–776.

Narihiro T, Hori T, Nagata O, Hoshino T, Yumoto I & Kamagata Y (2011) The impact of aridification and vegetation type on changes in the community structure of methane-cycling microorganisms in Japanese wetland soils. *Biosci Biotechnol Biochem* **75**: 1727–1734.

Nozhevnikova AN, Kotsyurbenko OR & Simankova MV (1994) Acetogenesis at low temperature. *Acetogenesis* (Drake HL, ed), pp. 416–431. Chapman & Hall, London, UK.

Oremland RS & Culbertson CW (1992) Importance of methane-oxidizing bacteria in the methane budget as revealed by the use of a specific inhibitor. *Nature* **356**: 421–423.

Pacheco-Oliver M, McDonald IR, Groleau D, Murrell JC & Miguez CB (2002) Detection of methanotrophs with highly divergent *pmoA* genes from Arctic soils. *FEMS Microbiol Lett* **209**: 313–319.

Popp TJ, Chanton JP, Whiting GJ & Grant N (2000) Evaluation of methane oxidation in the rhizosphere of *Carex* dominated fen in north central Alberta, Canada. *Biogeochemistry* **51**: 259–281.

Reeburgh WS, King JY, Regli SK, Kling GW, Auerbach NA & Walker DA (1998) A CH_4 emission estimate for the Kuparuk River basin, Alaska. *J Geophys Res* **103**: 29005–29014.

Saitou N & Nei N (1987) The neighbour-joining method – a new method for constructing phylogenetic trees. *Mol Biol Evol* **4**: 406–425.

Schloss PD & Handelsman J (2005) Introducing DOTUR, a computer program for defining operational taxonomic units and estimating species richness. *Appl Environ Microbiol* **71**: 1501–1506.

Semrau J, Chistoserdov A, Lebron J *et al.* (1995) Particulate methane monooxygenase genes in methanotrophs. *J Bacteriol* **177**: 3071–3079.

Siljanen HMP, Saari A, Krause S *et al.* (2011) Hydrology is reflected in the functioning and community composition of methanotrophs in the littoral wetland of a boreal lake. *FEMS Microbiol Ecol* **75**: 430–445.

Soil Survey Staff (1998) Natural Resources Conservation Service, United States Department of Agriculture. U.S. Soil Taxonomy. Available online at http://soildatamart.nrcs.usda.gov. [Accessed 09/15/2011].

Steinberg LM & Regan JM (2008) Phylogenetic comparison of the methanogenic communities from an acidic, oligotrophic fen and an anaerobic digester treating municipal wastewater sludge. *Appl Environ Microbiol* **74**: 6663–6671.

Ström L, Ekberg A, Mastepanov M & Christensen TR (2003) The effect of vascular plants on carbon turnover and methane emissions from a tundra wetland. *Global Change Biol* **9**: 1185–1192.

Tamura K, Peterson D, Peterson N, Stecher G, Nei M & Kumar S (2011) MEGA5: molecular evolutionary genetics analysis using maximum likelihood, evolutionary distance, and maximum parsimony methods. *Mol Biol Evol* **28**: 2731–2739.

Tarnocai C, Canadell JG, Schuur EAG, Kuhry P, Mazhitova G & Zimov S (2009) Soil organic carbon pools in the northern circumpolar permafrost region. *Global Biogeochem Cycles* **23**: 1–11.

Thauer RK (1998) Biochemistry of methanogenesis: a tribute to Marjory Stephenson. *Microbiology* **144**: 2377–2406.

Theisen AR & Murrell JC (2005) Facultative methanotrophs revisited. *J Bacteriol* **187**: 4303–4305.

Trotsenko Y & Khmelenina V (2002) Biology of extremophilic and extremotolerant methanotrophs. *Arch Microbiol* **177**: 123.

van Everdingen RO (ed) (2005) *Multi-Language Glossary of Permafrost and Related Ground-Ice Terms*. International Permafrost Association, University of Calgary, Calgary, AB, Canada. (Available at http://nsidc.org/fgdc/glossary)

Wagner D & Liebner S (2009) Global warming and carbon dynamics in permafrost soils: methane production and oxidation. *Permafrost Soils*, Vol. **16** (Margesin R, ed), pp. 219–236. Springer, Berlin, Heidelberg.

Wagner D & Liebner S (2010) Methanogenesis in arctic permafrost habitats. *Handbook of Hydrocarbon and Lipid Microbiology* (Timmis KN, ed), pp. 666–663. Springer-Verlag, Berlin, Heidelberg, Germany.

Wagner D, Kobabe S, Pfeiffer EM & Hubberten HW (2003) Microbial controls on methane fluxes from a polygonal tundra of the Lena Delta, Siberia. *Permafrost Periglac* **14**: 173–185.

Wagner D, Gattinger A, Embacher A, Pfeiffer EM, Schloter M & Lipski A (2007) Methanogenic activity and biomass in Holocene permafrost deposits of the Lena Delta, Siberian Arctic and its implication for the global methane budge. *Glob Change Biol* **13**: 1089–1099.

Wartiainen I, Hestnes AG & Svenning MM (2003) Methanotrophic diversity in high arctic wetlands on the islands of svalbard (Norway) – denaturing gradient gel electrophoresis analysis of soil DNA and enrichment cultures. *Can J Microbiol* **49**: 602–612.

Wartiainen I, Hestnes AG, Mcdonald IR & Svenning MM (2006) *Methylobacter tundripaludum* sp. nov., a methane-oxidizing bacterium from arctic wetland soil on the Svalbard islands, Norway (78°N). *Int J Syst Evol Microbiol* **56**: 109–113.

Whalen SC & Reeburgh WS (1992) Interannual variations in tundra methane emission: a 4-year time series at fixed sites. *Global Biogeochem Cycles* **6**: 139–159.

Whalen SC, Reeburgh WS & Sandbeck KA (1990) Rapid methane oxidation in a landfill cover soil. *Appl Environ Microbiol* **56**: 3405–3411.

Wille C, Kutzbach L, Sachs T, Wagner D & Pfeiffer E-M (2008) Methane emission from Siberian arctic polygonal tundra: eddy covariance measurements and modeling. *Glob Change Biol* **14**: 1395–1408.

Yergeau E, Hogues H, Whyte LG & Greer CW (2010) The functional potential of high Arctic permafrost revealed by metagenomic sequencing, qPCR and microarray analyses. *ISME J* **4**: 1206–1214.

Yrjälä K, Tuomivirta TT, Juottonen H, Putkinen A, Tuittila ES, Penttil T, Laine J, Peltoniemi K & Fritze H (2011) CH_4 production and oxidation processes in a boreal fen ecosystem after long-term water table drawdown. *Glob Change Biol* **17**: 1311–1320.

Supporting Information

Additional Supporting Information may be found in the online version of this article:

Fig. S1. Rarefaction curves of (a) McrA sequences of methanogenic archaea and (b) PmoA sequences of methane oxidizing bacteria using a cutoff value of 14.3% and 7% respectively, from active layer samples of Herschel Island, Canadian Western Arctic.

Please note: Wiley-Blackwell is not responsible for the content or functionality of any supporting materials supplied by the authors. Any queries (other than missing material) should be directed to the corresponding author for the article.